

Electromagnetic Emission from “Dielectric” Optical Fiber Cables

Robert Dahlgren
Silicon Valley Photonics, Ltd.
PO Box 1569, San Jose, CA 95109
http://www.svphotonics.com
bob@svphotonics.com +1 (408) 437-9292

Prof. Zorica Pantic-Tanner
Dept. of Electrical Engineering
University of Texas at San Antonio
6900 N. Loop Road, San Antonio, TX 78249
zptanner@utsa.edu +1 (210) 458-7379

Abstract

The conventional wisdom is that optical fiber is dielectric, and thus does not radiate RF emissions. In practice, optical fiber cable connectors have non-negligible amounts of conductive material, for example a ferrule, spring, and crimp ring. As data rates have increased beyond 1 gigabit/second (Gbps), equipment with supposedly “RF tight” enclosures exhibited high levels of RF emissions, failing to meet FCC/European electromagnetic compliance (EMC) requirements. It is hypothesized that these small metallic bits can re-radiate RF emissions due to capacitive coupling, and a model is proposed. Data is presented to support this mechanism for RF emission, and corrective measures are suggested to reduce these emissions.

1. Introduction

High-speed data links have enabled networking technology and new system architectures, such as distributed storage. Figure 1 illustrates a typical datacom application, in this example the physical decoupling of a PC workstation and mass storage. A host adapter card (HAC) provides the optical fiber interface from the workstation via, for example, the PCI bus. An example of mass storage equipment would be a redundant array of independent disks (RAID) with its controller/ interface. Initially, the data links were based upon metallic cable technology such as SCSI and Ethernet. These “copper” solutions have well-known rate, distance, EMC, and topological limitations.

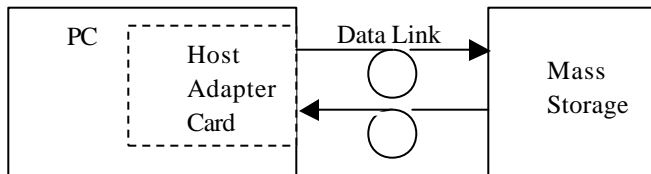


Figure 1. Workstation with Data Link and Mass Storage.

Common physical enclosures include “pizza-box,” tower, or rack-mounted styles, and are always electrically shielded in some manner. There is no loss of generality if we consider this simple topology and a reduced set of network equipment. The same physics and design issues apply equally to gigabit switch, hub and other equipment for both telecom and datacom implementations.

The evolution of optical data link industry from a telecom (WAN) to a datacom (LAN) market has spawned long-distance gigabit data links with $<10^{-12}$ bit error rates, at costs approaching parity with copper media in some cases. Importantly, fiber optics has a reputation of having zero EMC emissions, because it is made of glass, which is a dielectric. Furthermore, robust cable that incorporates optical fiber can be manufactured out of dielectrics such as PVC, silicone, and Kevlar™ aramid fiber. Systems using optical fiber cable are less susceptible to external ESD and RF fields, and are extremely difficult to tap: electrical shielding of the cable is unnecessary. Non-metallic cables are also exempt from conducted immunity and conducted emissions testing, further reducing the regulatory burden. For these reasons, optical fiber is the high-speed media of choice for all but the shortest-distance data links. The distance for an optical data link could be two meters for a desktop application, or many kilometers for a remote database application.

2. Problem

System designers were aware that as serial transmission rates (and rise/fall times) increased, the amount of high frequency RF components generated by the system increased. An enclosure design that passes EMC tests with good margin at 10 Mbps could be wholly unsuitable for a 100× increase of data rate. System designers and EMC compliance engineers thought that by continuing to design enclosures such that they were RF-tight, EMC compliance could easily be achieved [1]. The thinking was fiber, being a dielectric, would not be able to radiate RF emissions.

It is well known that an aperture will not radiate RF emissions of frequency f , if the frequency is below the so-called cutoff frequency f_c . At this frequency, the wavelength of the RF emissions is such that the aperture size is equal to one-half wavelength [2]. For an ideal enclosure with an aperture of size D , cutoff wavelength Λ_c is found by setting $D = \Lambda_c/2$

$$\Lambda_c = 2D \quad \text{and substituting}$$

$$\Lambda = c/f \quad c \cong 3 \times 10^8 \text{ meters/sec in air}$$

yields the cutoff frequency of an air-filled aperture

$$f_c = c/\Lambda_c = c/2D$$

Where D corresponds to the maximum dimension on an arbitrary aperture in an ideal planar conductor, e.g. the diagonal of a rectangular aperture. Simply stated, Maxwell's equations predicts that only evanescent (bound) fields exist for $f > c/2D$ only, in the immediate vicinity of the aperture. There would be no radiating field solution for Maxwell's equations, and no RF emission [3]. An RF-tight enclosure could be engineered for $f < f_c$ by limiting the number, size, and design of louvers, slots, seams, cable feedthroughs, ventilation holes and other apertures penetrating the shielding enclosure.

To pass FCC requirements the 5th harmonic of the maximum frequency must be considered. There is also a strong emission peak associated in serial data link systems at half the bit rate, which corresponds to the 101010... data pattern, and at the byte clock frequencies (usually 1/10 or 1/8 of the bit rate), and any other strong RF sources in the system. Often the 3rd, 5th, and 7th harmonics are problematic. The standards committees and early adopters of this technology took these into consideration when specifying the physical nature of these interconnects. Design rules were revised which limited connector and panel aperture size accordingly.

D Estimated Aperture Size	Example Fiber Connector	f_c Maximum RF Frequency Contained
28 mm	Duplex-SC	5.4 GHz
14 mm	Simplex-SC *	10.7 GHz
11 mm	MT-RJ	14 GHz
5.0 mm	2 × SC ferrule	30 GHz
2.5 mm	2 × LC ferrule	60 GHz

* or duplex-SC with septum [3]

For example, IEEE 802.3z Ethernet specifies a nominal bit rate of 1.25 Gbps, which would suggest a 5th harmonic at 3.125 GHz and 7th harmonic near 4.375 GHz, easily contained by a 28 mm aperture. However, those systems integrators who were the early adopters of gigabit optical technology found that first production samples failed EMC tests. In some cases, large RF emissions were observed for theoretically RF-tight enclosures, even when the apertures in the enclosure were significantly smaller than would correspond to the failing frequency. This caused equipment vendors to suffer schedule delays in the early 1990s.

3. Observations and Serendipity

During prototype EMC testing of datacom equipment employing 1.0625 Gbps optical data links, failures were commonplace in the 500 MHz to 4 GHz range. In one case, a RAID system used duplex-SC connectors ($D=28$ mm), and was emitting RF energy in some cases 20 dB over the Class B limit. This was especially baffling because EMC failures occurred at frequencies well below the cutoff frequency - everything from DC up to 5.4 GHz should be suppressed to a high degree!

The EMC test configuration at an open-air test site (OATS) was similar to Figure 2, with the RAID system sitting on the EMC test turntable, connected to a 100-meter optical fiber cable. The OATS facility employed calibrated antennae and RF

spectrum analyzers in the remotely located control room to measure RF emissions per the EMC test protocols. The PC workstation was placed outside of the range of the OATS, and a bitstream consisting of idle and data characters was transmitted bi-directionally between the two systems.

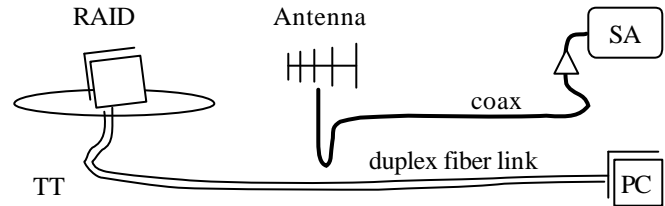


Figure 2. OATS showing RAID box on turntable (TT) and spectrum analyzer (SA) in control room (not to scale).

The author was working on the OATS turntable, watching a particularly troublesome EMC failure peak ($f \approx 1.6$ GHz) on the RF spectrum analyzer. When the data link was in operation, the RF emission at this particular frequency was well above the legal limit. When the optical fiber cable was unplugged from the RAID system, that RF emission peak dropped to baseline levels, indicating that the enclosure was RF-tight.

While the fiber was unplugged, the same spectral peak was observed with an RF near-field probe, which detected the evanescent (non-radiating) field in the immediate vicinity of the aperture. This demonstrated that there was 1.6-GHz RF energy inside the enclosure, and that aperture was below cutoff and functioning to contain the RF energy.

One strange observation was that when the fiber cable was unplugged from the PC workstation (located well outside of the OATS) the emissions dropped by a much lesser amount than when it was unplugged from the RAID box. If the fiber was truly a dielectric, the numbers had to be the same, according to cutoff theory. This was pondered while subconsciously tapping a small screwdriver near the RAID system, when it was noticed the level of the emissions peak on the spectrum analyzer was dancing in unison with the screwdriver motion. When the screwdriver was brought near the aperture, the emissions rose sharply, and decreased to baseline levels as it was removed. Could metal near the aperture be the cause of the radiation? Closer examination of some optical connectors revealed conductive sub-components such as a ferrule body, a crimp ring, a small spring, etc. Even though the fiber cable itself is dielectric, the minuscule metallic bits in the connectors, being near the aperture, somehow drastically contributed to the radiated emissions. Reference [4] suggests that conductive bodies act as flux concentrators that reduce shielding effectiveness.

4. Emissions Model

Refer to Figure 3, which illustrates a simplified physical layout common in data link host systems. Within the conductive, grounded enclosure, there is a motherboard (PCB1) and a HAC daughtercard (PCB2). In between the PCBs

are various connectors, the type is not important. However, parasitic effects such as capacitance and particularly inductance are important to this model. There could be more levels, e.g. a transceiver module mounted on the HAC has PCB3 and its own connector, but this 2-level model is sufficient for understanding. Consider the high-frequency currents flowing through the decidedly non-ideal connectors. In the GHz regime, a small inductance can have significant positive reactance (1 nH at 1 GHz equals approximately $+6j$ ohms). This finite reactance leads to finite potential differences between PCB1 and PCB2 and the enclosure, as indicated by the + and - at L1 and L2. It is believed that the ground planes dominate the radiation model, because they present the most surface area (i.e. are the biggest antenna).

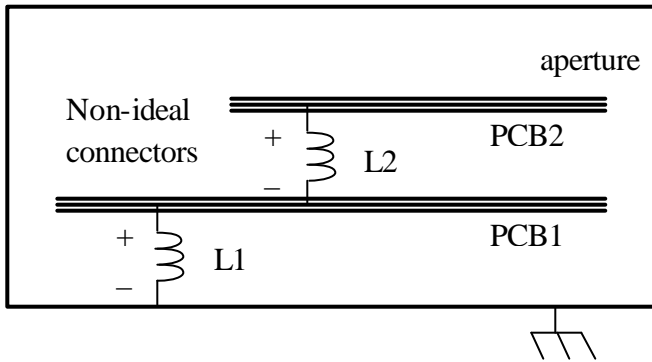


Figure 3. Simplified layout of system ground plane stack-up.

It is usually possible to ground the motherboard with low-impedance techniques, so neglect L1 and consider the voltage difference between the ground planes across L2. Other EMI sources such as high frequency ICs, current-loops, and clock distribution, while very important, are beyond the scope of this discussion.

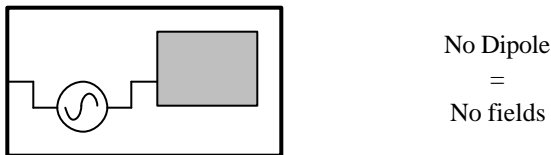


Figure 4A. Ideal enclosure with RF voltage source.

In this simple model, the inductance is replaced by a Thévenin equivalent voltage source at frequency f , between PCB2 and the enclosure shield. Figure 4A illustrates a single ground plane EMI source inside an ideal enclosure with no aperture. There is no radiation, because the inside half of the dipole antenna is completely shielded, due to the ideal Faraday cage; and an electrical monopole does not radiate.

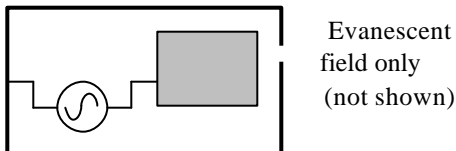


Figure 4B. Ideal enclosure with small aperture.

Figure 4B is the same ideal enclosure with a small aperture. For any frequencies f below f_c the non-radiative evanescent field exists only a few mm from the aperture, and the RF energy is theoretically contained within the enclosure. This is when the fiber is unplugged from the RAID system.

Figure 4C shows the same ideal enclosure with a small conductive element outside the enclosure, in the vicinity of the aperture, such as would be introduced by metal in an optical fiber connector (or an errant screwdriver). It is hypothesized that there is a finite parasitic capacitive coupling between the ground plane inside the enclosure, and the metallic body, through the aperture. The interested reader may calculate the capacitance between two planes imaged through a grounded aperture using Green's functions [5].

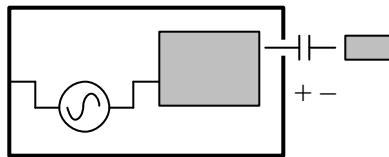


Figure 4C. Ideal enclosure with metallic body near aperture.

In this case there is the evanescent field as before, but the metallic body will experience a driving voltage via the parasitic capacitance as shown by the + and -. Recall that at GHz frequencies, 1 pF presents low impedance, even though the metallic body is physically separated from the aperture.

Figure 4D shows the resultant equivalent circuit, where again the voltage across a parasitic element is represented by an equivalent Thévenin voltage source of the proper frequency and impedance. This in effect creates a new dipole radiator, with the enclosure as one half of the dipole, and the metallic body as the other (albeit much smaller) half of the dipole radiator.

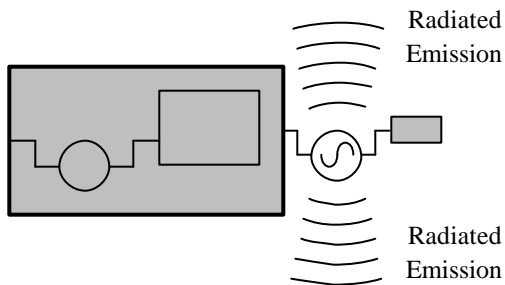


Figure 4D. Resultant equivalent dipole model.

Another way to look at it is that emissions occur because a small fraction of the formerly well-shielded dipole is now outside of the enclosure. This illustrates a possible mechanism of RF emission for enclosures with sub-cutoff apertures: The capacitive coupling between a driven internal ground plane and the outside world induces a voltage difference between any conductive item in the vicinity of the aperture.

5. Experiment

A test enclosure with a simplified arrangement corresponding to Figure 3 was constructed, using a large Bud box, copper-clad PCB material, a crystal oscillator, voltage regulator, and a 9-volt battery, with a circuit similar to [6]. The motherboard was heavily grounded to the chassis with multiple aluminum stand-offs. In this manner we neglect L1 and the voltage between the motherboard and the enclosure. The oscillator on PCB1 drove a mismatched load on PCB2 (to get a maximum emissions), via a 4x12 pin connector. The specification for the apparatus is listed below.

Enclosure Size	20 cm x 30 cm x 28 cm
Enclosure Type	Steel box, sheet metal screws
Oscillator Type	Ecliptek E1100
Frequency	160 MHz
Edge Rate	1.1 nsec
Aperture Size	28 mm x 12 mm
Daughter Card Size	50 mm x 200 mm
Daughter Card to Aperture	28 mm
Connector	3M 48-pin

The edge rate corresponds to frequency components slightly below 1 GHz. The daughter card ground plane is brought close to the aperture inside the test enclosure, like the panel of a typical datacom system or HAC.

The EMC measurements were taken at the Rolm Electronics 10-meter semi-anechoic chamber in Santa Clara, California. Measurement uncertainty of the test setup is approximately ± 4 dB.

5.1 Evanescent radiation.

Battery power was applied to the oscillator, and the test enclosure was placed on the turntable with the open aperture facing 0° . To make sure the cutoff phenomenon was in effect, a baseline measurement was done. The turntable was rotated to find maximum emissions near 20° , and the emission spectrum is reproduced in Figure 5. Note the 957 MHz peak, there is a 20 dB margin below FCC class A requirements. The presence of the 957 MHz evanescent field was then verified using a near-field probe.

5.2 Metallic Body Present

A small wire, #24 AWG and approximately 50 mm long, was placed perpendicular to the aperture, coupled with approximately 10 pF to the daughter card ground plane. The EMI was re-measured in the same manner as before, and is shown as Figure 6. In this test, nearly the same low value is observed as in Figure 5.

Rotating the test enclosure to an angle of 89° results in maximum emissions detected, at the major radiation lobe. This is near the theoretical maximum for an ideal dipole radiator, 90° from its axis of symmetry, as one expects for a dipole radiation model. The emission spectrum is shown in Figure 7, where the emissions peak increases by over 12 dB from the baseline measurements. Although this emission level would pass class A, it would not be sufficient to meet class B requirements. This

experiment replicates the anomalous emission observed in the OATS, and behaves as predicted by the driven-dipole model.

If the 10 pF capacitor is removed, while leaving the metallic body in place, the emissions are observed to drop significantly. This illustrates the role of capacitive coupling between the internal ground plane and the external world.

5.3 Confirmation of Driving Source

To verify that a voltage source is driving the metallic body via the capacitance, which generates emissions, and not some electromagnetic phenomena, the PCB is grounded right near the aperture, not just through the 48-pin connector. In this test, copper tape was used to run from the daughter card ground to the test enclosure ground, immediately adjacent to the aperture. This provides a low-impedance path, essentially shorting out the voltage source. Figure 8 is an emission spectrum for this situation, with the wire and 10 pF coupling capacitor in place as before. Note that when there is no voltage to drive the capacitance to objects in the outside world, there are also low emissions. This verifies that the PCB2 ground plane is driving the metal objects in the fiber optic connector, via parasitic capacitive coupling.

5.4 Role of Parasitic Inductance

Figures 9 through 11 are a series of emission spectra, taken with the 10 pF capacitor and metallic body present, to illustrate the role of connector parasitic inductance to the model. Figure 9 is an emissions spectrum, where a single ground pin is used to cascade the ground planes, having roughly 10 nH of inductance. Figure 10 is the same test repeated, with 10 ground pins connecting the daughtercard to the motherboard. At the 950 MHz peaks, there is an observed 8 dB reduction in emissions. In Figure 11, there are 40 out of 48 pins used to connect the PCB1 and PCB2 ground planes together, showing an even better 15 dB improvement over the baseline. This is summarized in the table below.

PCB1-PCB2 Signal Pins	PCB1-PCB2 Ground Pins	RF Emissions at 961 MHz
1	1	43.2 db μ V/m
1	10	34.9 db μ V/m
1	40	27.9 db μ V/m

The net inductance does not scale as $1/N$, but has self-inductance, mutual inductance, and geometric effects which cause a much lesser reduction in net inductance than $1/N$. The point of this experiment is to indicate the importance of adequate grounding of PCB stacks, and verify the hypothesis of the ultimate source of the driving energy.

6. Conclusions

The conclusion of this study is that when new technology and/or higher clock frequencies are applied to present EMC enclosures and design methodologies, there may be unforeseen non-idealities that cause EMC failures. In this case, forgotten metallic parts in an otherwise totally dielectric medium caused the system as a whole to fail EMI. A possible model for emission has been proposed and confirmed.

Although system EMC performance must be confirmed by rigorous testing, some design practices that could be inferred from this study include:

- In general, make aperture size small, the smaller the better. Not only does this raise the cutoff frequency, but also its shielding effect reduces parasitic capacitance to the outside world.
- Use a conductive dust cover, or a “trap door” with a good EMC gasket that automatically covers fiber-optic apertures when not in use.
- Do not underestimate the precision required to obtain consistent low-impedance ground connections, particularly with respect to front-panel-to-daughtercard tolerancing.
- Minimize the surface area of daughter card and module shielding inside the enclosure near the aperture. This reduces parasitic capacitance to the outside world.
- Maximize the distance between the daughter card and other PCBs to the aperture.
- By that same token, maximize the distance between any metallic bodies (e.g. a laser diode TO-can) in a fiber-optic receptacle and the aperture. This has the added benefit of increasing immunity to ESD and external RF fields, due to the theory of reciprocity.
- Minimize or eliminate conductive materials in fiber optic connectors. One technique proposed is replacing the metal spring with an elastomeric spring.
- Use homogeneous ground techniques when possible. Tie the ground planes to the chassis at as many points as possible, using conductive “fingerstock” or other low-impedance techniques.
- Use as many ground pins and auxiliary grounding techniques as possible in motherboard-to-daughtercard connections. This also reduces potential differences within the enclosure. As a bonus, it results in better board-to-board signal integrity.
- The Vcc plane(s) should have ultra-low impedance over as wide a frequency range as possible, through liberal use of bypass capacitors and ferrites.
- For duplex fiber receptacles, if possible, add a conductive septum or otherwise subdivide the aperture [4].
- Optical module shielding with low impedance continuity to the system enclosure may be effective. For example, blocking the faceplate aperture with a continuous shield, leaving a minimal internal aperture(s) for the fiber itself.

- Incorporate shielding with low impedance continuity to the system enclosure, surrounding the backside of the module body. This works particularly well with removable “hot pluggable” optical modules.
- Pay careful consideration to arrayed apertures. A rule of thumb is that shielding effectiveness will be reduced between $10\log N$ and $20\log N$ where N is the number of apertures enclosed within a diameter of Λ [7].
- Do not route critical high-frequency transmission lines on the surface of a PCB. When possible, route these in between internal ground planes. Control and minimize the area of high-frequency current loops, and follow IC manufacturers’ bypassing recommendations.

7. Acknowledgments

The authors would like to thank San Jose State University, San Francisco State University, Rolm Electronics, Fujikura Technology, Ken Renda, Franz Gisin, Lee Hill, Ron Kleckowski, and Francisco DeAnda.

8. References

1. Dahlgren, Robert P., “EMI Radiation from sub-1/2 Wavelength Apertures,” *SJSU EE296F Class Project* (1995).
2. Ott, Henry W., Noise Reduction Techniques in Electronic Systems, Wiley (1998).
3. There can be some small RF emissions due to waveguide effects, but they are negligible and beyond the scope of this discussion.
4. Masterson, Keith D., *et al*, “Electromagnetic Shielding Characteristics of Optical-Fiber Connectors,” *NIST Technical Note 1383*, (1997).
5. Jackson, John D., Classical Electrodynamics, Wiley (1975).
6. Robinson, Martin P., *et al*, “Analytical Formulation for the Shielding Effectiveness of Enclosures with Apertures,” *IEEE Trans. Electromagnetic Compatibility*, Vol. 40, No. 3, (August 1998), pp 240-248.
7. Brewer, Ron., “Design Considerations for Minimizing Large Aperture Effects in Shielding,” *ITEM*, (2002) pp138-144.

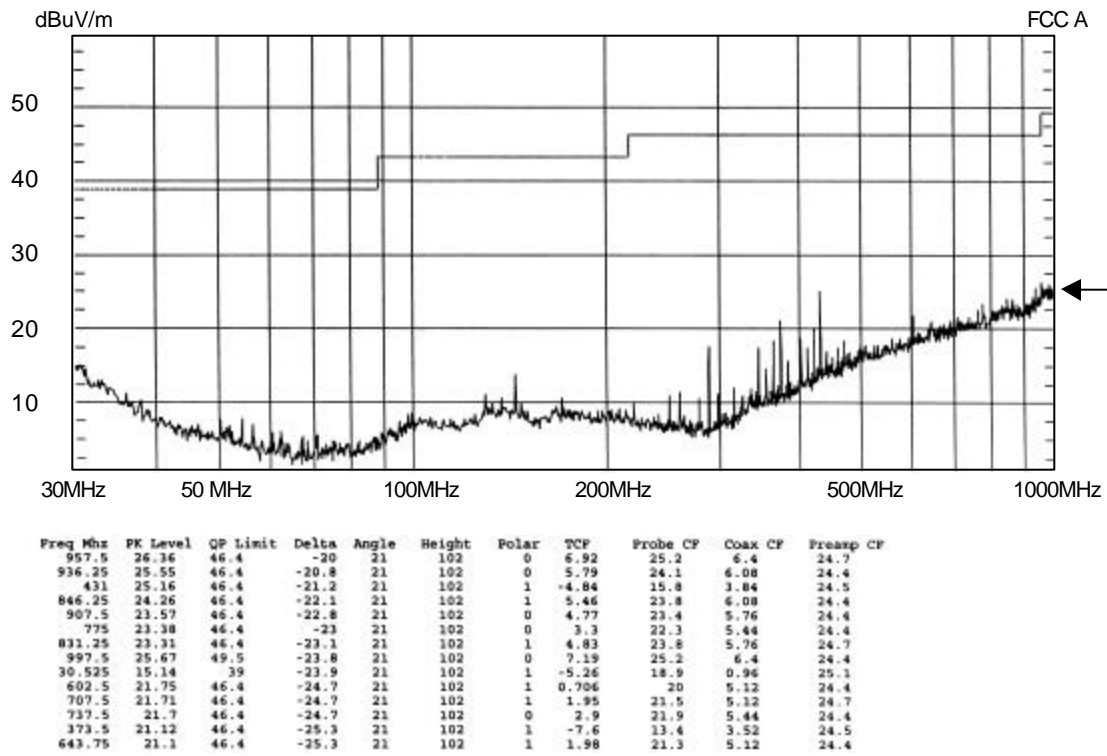


Figure 5. Baseline measurement. No external metallic body present. Emission 20.0 dB below FCC class A limit.

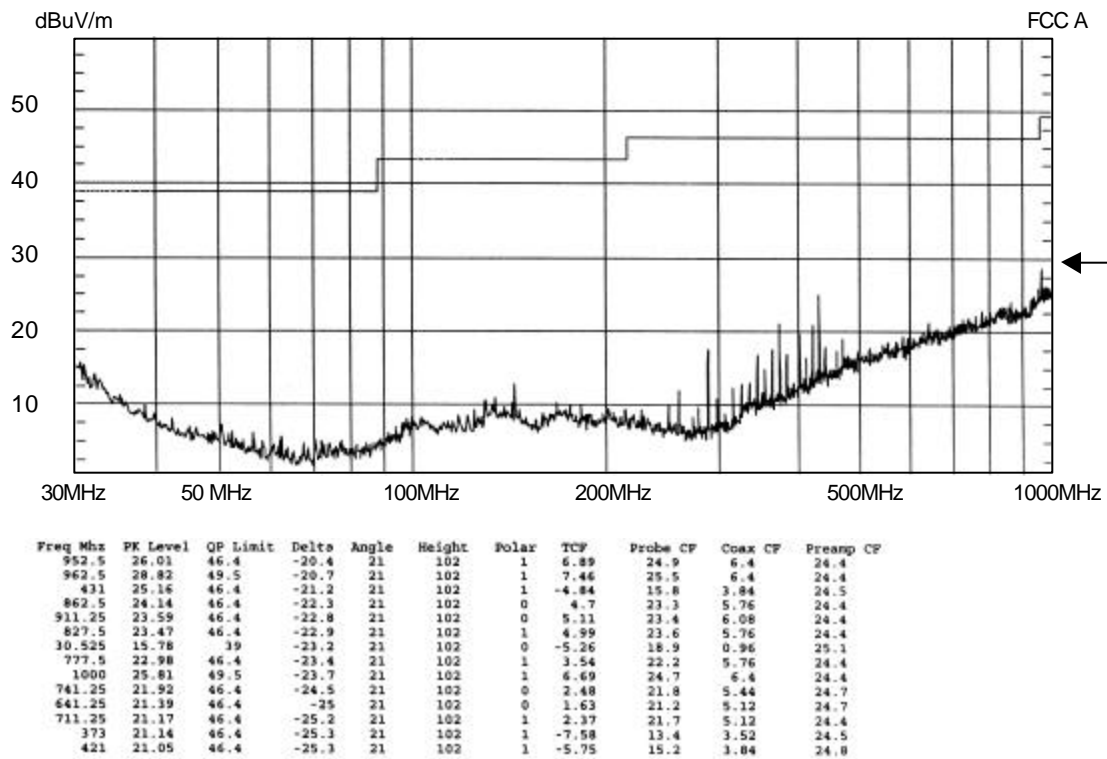


Figure 6. Metallic body present with 10-pF coupling. Emission 20.4 dB below FCC class A limit, ~20° off-axis.

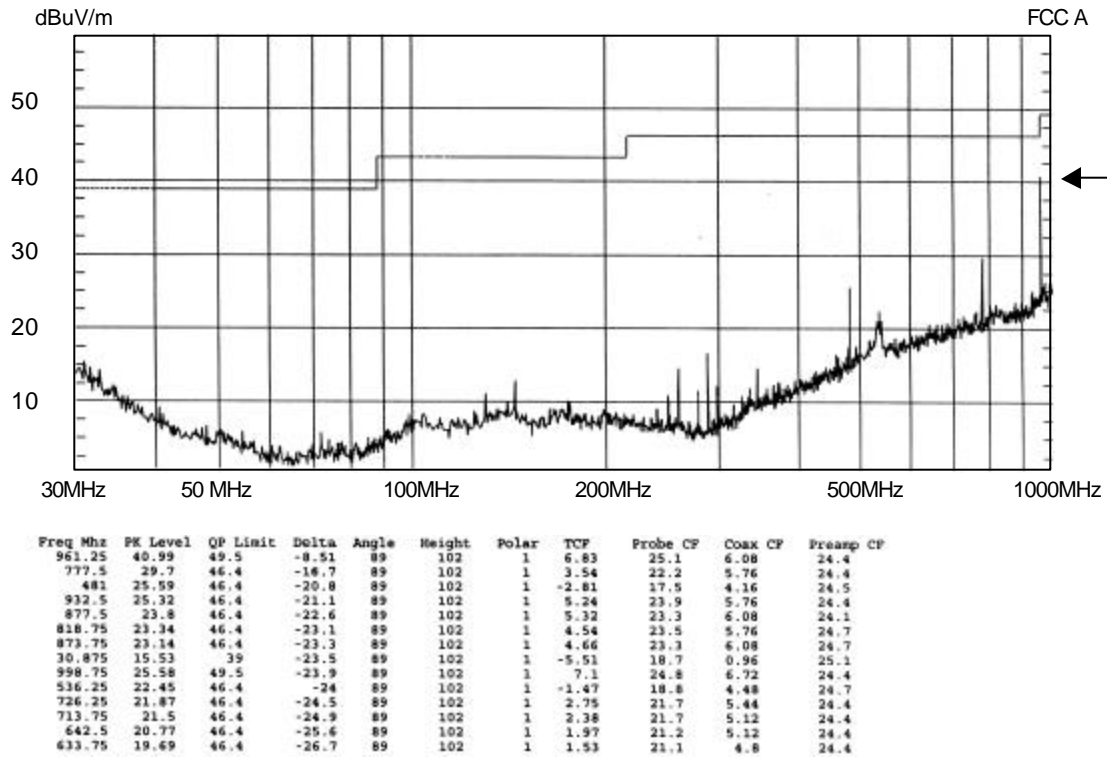


Figure 7. Metallic body present with 10-pF coupling. Emission 8.5 dB below FCC class A limit, ~90° off-axis.

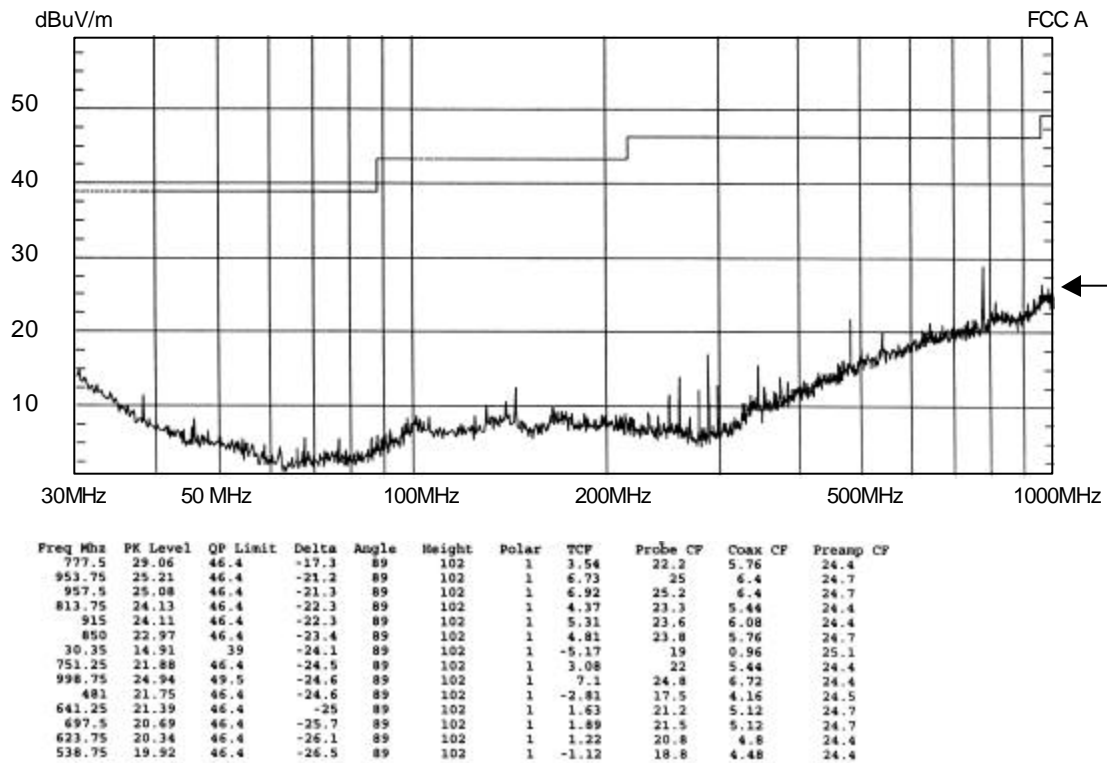


Figure 8. Confirm driving source. Daughtercard shorted to ground. Emission 21.2 dB below FCC class A level.

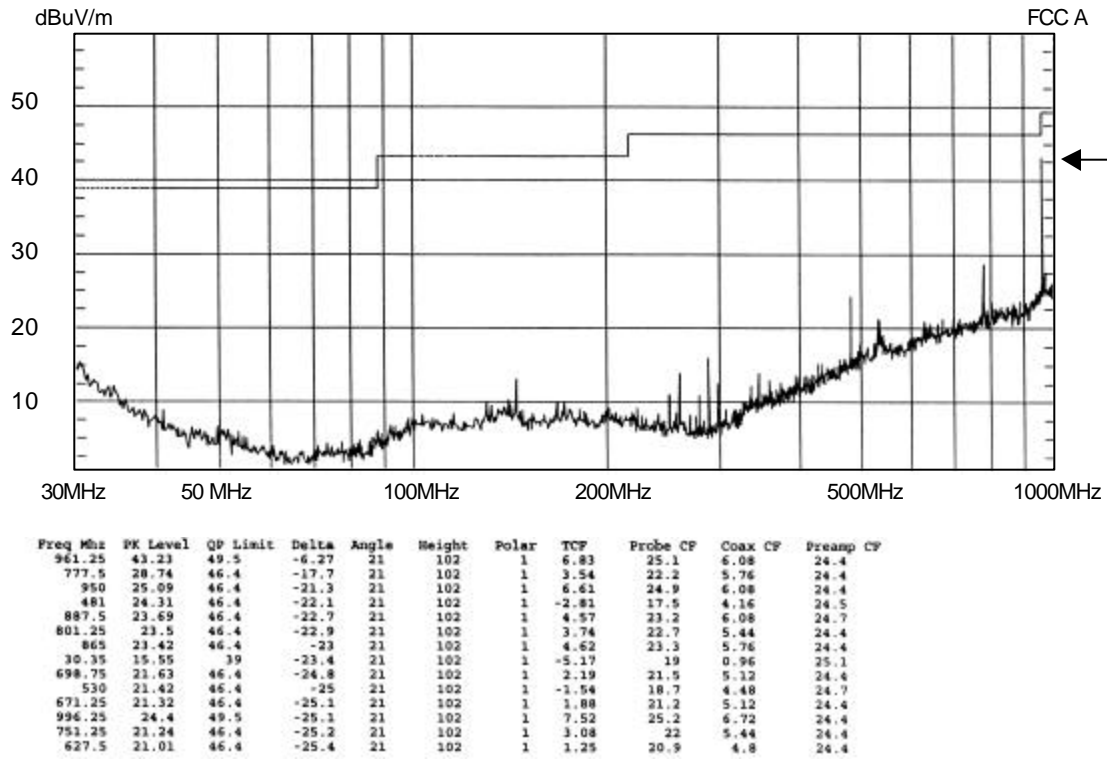


Figure 9. High connector inductance. Ground pin 1:48 ratio. Emission 6.3 dB below FCC class A.

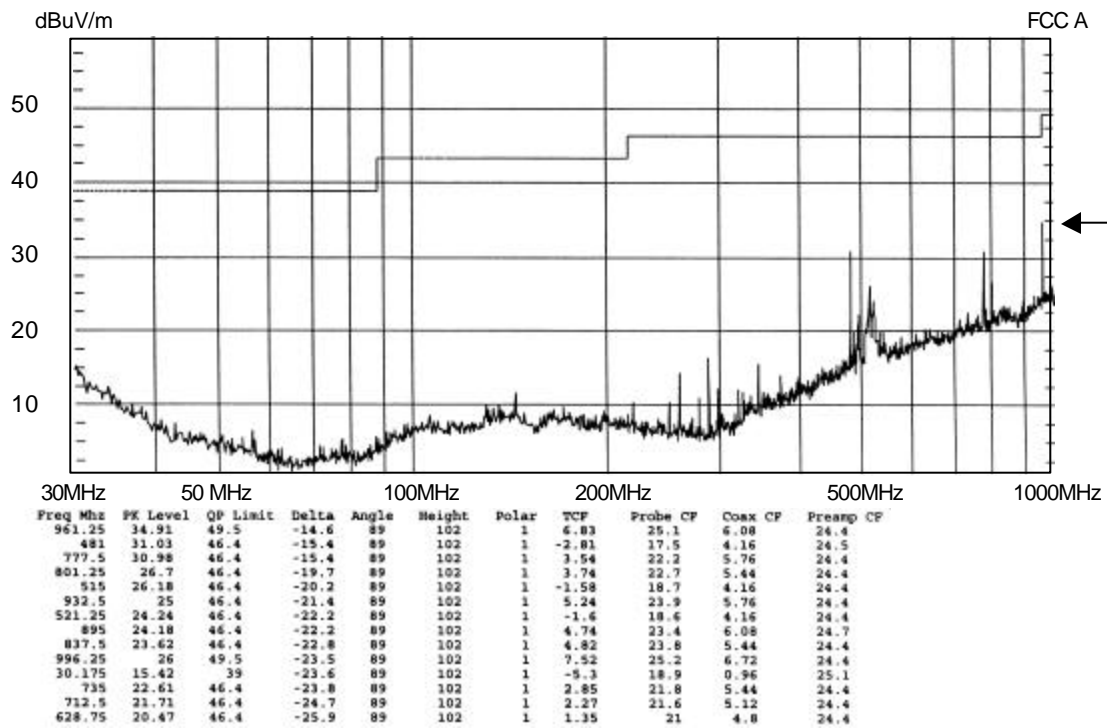


Figure 10. Medium connector inductance. Ground pins 10:48 ratio. Emission 14.6 dB below FCC class A.

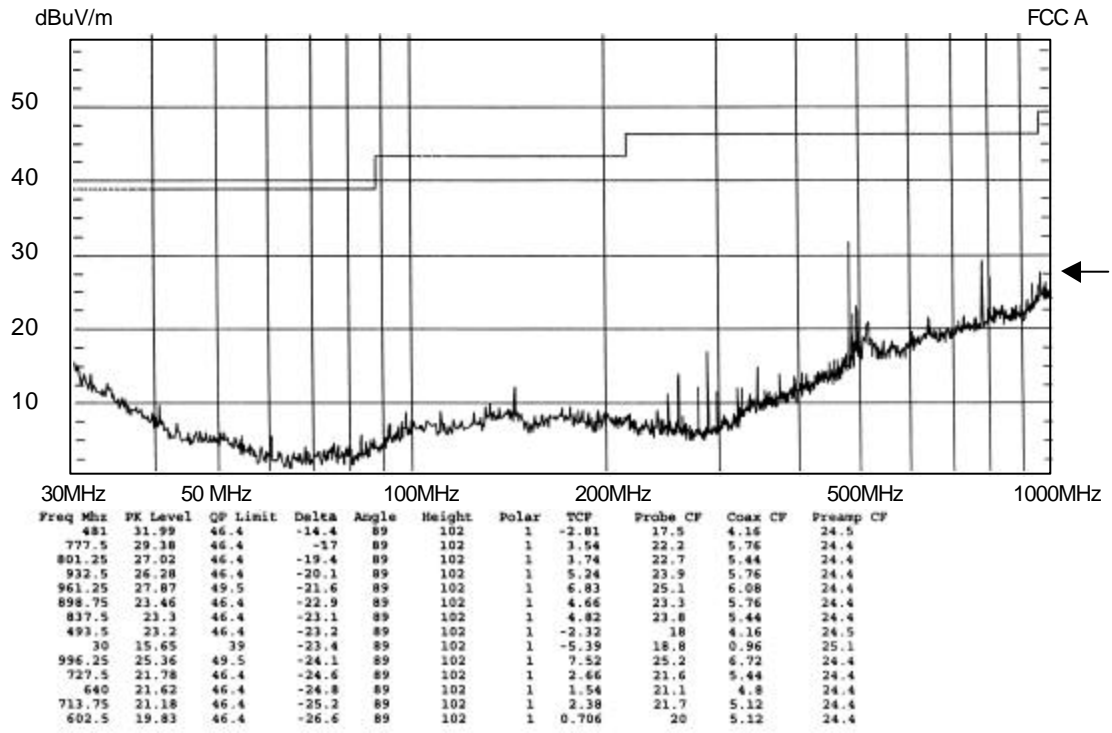


Figure 11. Low connector inductance. Ground pins 40:48 ratio. Emission 22.6 dB below FCC class A.